Modeling Coronal Mass Ejections*

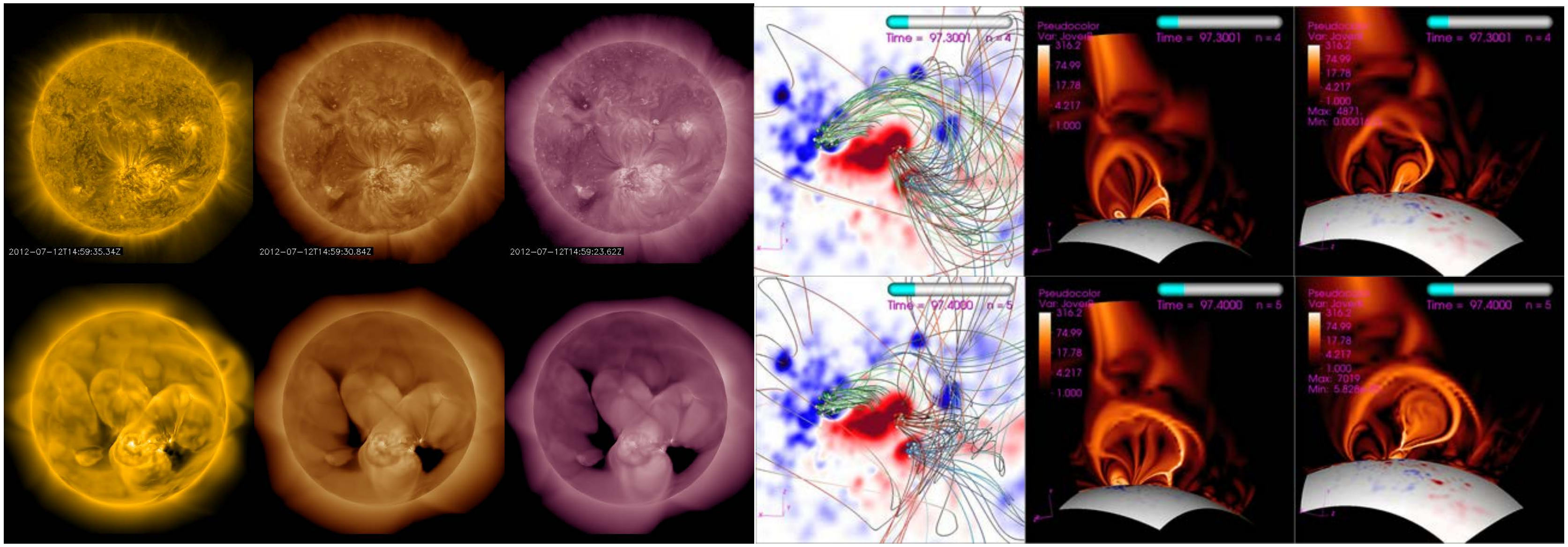

Jon A. Linker, Cooper Downs, Tibor Torok, Viacheslav Titov, Roberto Lionello, Zoran Mikic, Ronald M. Caplan, and Pete Riley

Predictive Science Inc. (PSI), San Diego, CA, USA

Nathan Schwadron & Matthew Gorby

University of New Hampshire, Durham, NH, USA

*Research Supported by NASA, AFOSR & NSF

Introduction

- An open question regarding CMEs is the nature and origin of the highly non-potential magnetic fields that are the source of their energy
- We want also want to understand phenomena related to CMEs, e.g.:
  - Evolution and propagation of CMEs
  - Acceleration/transport of solar energetic particles (SEPs)
- In many cases we would like to defer the first question and study the succeeding questions, many of which are important for space weather
- Practically, we want to perform realistic CME simulations that start from a configuration that is already close to eruption, but in equilibrium.
- The Titov & Demoulin (1999) Model: an analytic model of a flux rope equilibrium used in previous simulations
- We want a model that takes into account the background magnetic field of our simulation.
- We developed a new (TDm) model: Titov et al. *Astrophys. J.* 2014.

Simulating CMEs: Key Elements

- "Realistic" model of the solar corona:
  - Based on observed magnetic fields (magnetograms)
  - Includes transition region, energy physics (necessary for comparing with EUV)
- When initiating CMEs, preserve observed magnetic flux distribution as much as possible:
  - The streamer structure is the part of the model most tied to observations
  - We need both background streamer field and CME flux rope for low coronal phenomena
  - CMEs at 1 AU are a combination of both
- Destabilize from equilibrium configurations:
  - Important for studying EUV waves, dimming, etc.
  - May be crucial for flux rope rotation
  - Nonequilibrium simulations can be useful for some applications

Example:

- We have used TDm flux ropes to model an "extreme" event
  - July 14, 2000 "Bastille Day" CME
  - Demonstrated significant energy storage and release (> 10^{33} ergs)
  - Magnetic flux rope propagation to 1 AU
  - SEP acceleration and propagation

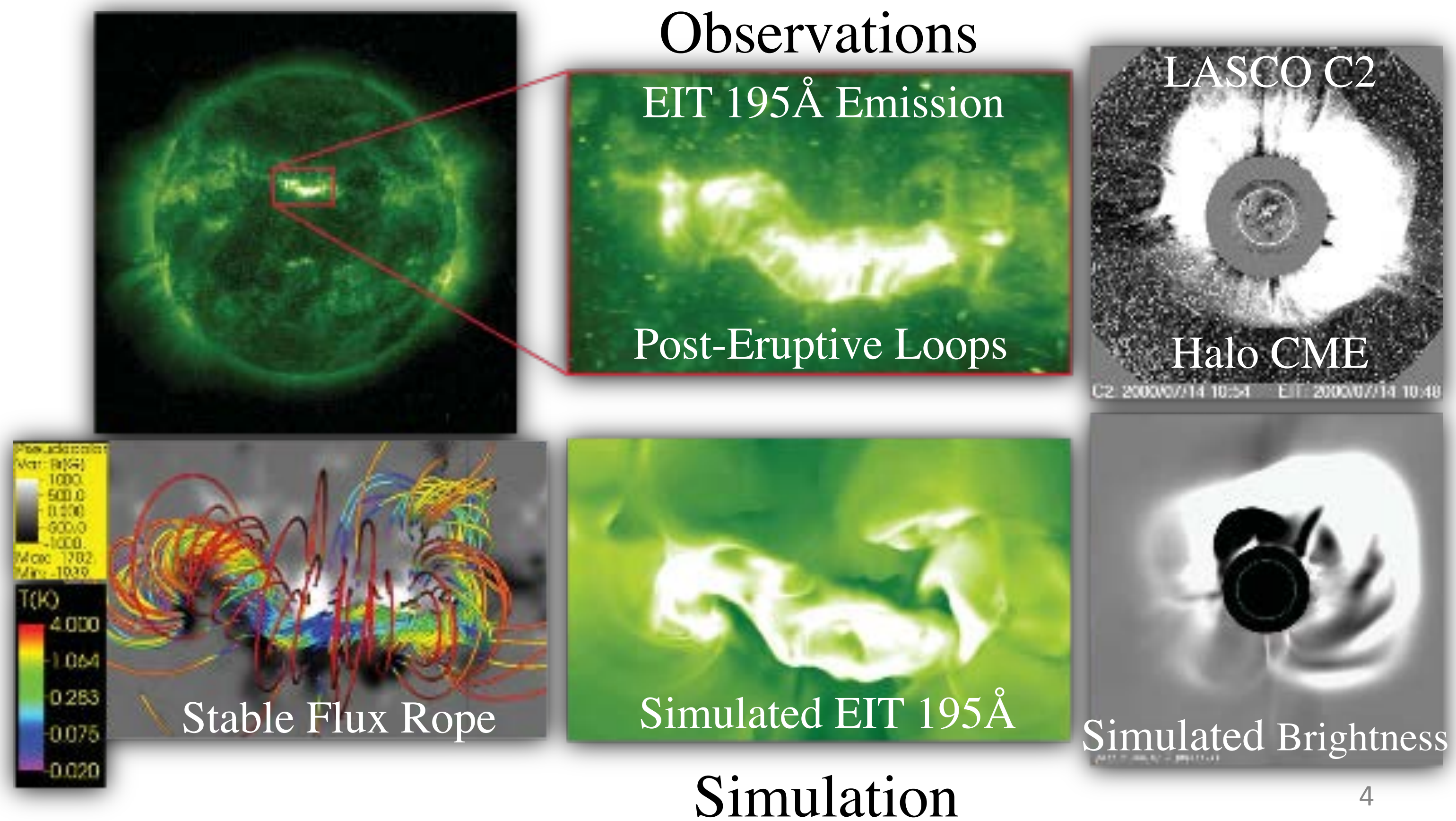

July 12, 2012 CME

- X1.4 Flare, Fast CME from a complex active region (AR11520)
- Triggered large geomagnetic storm (DST = -127nT)
- SEPs observed at STEREO and ACE
- This active region later produced the July 23 solar superstorm

12 July 2012: A Complex Multipolar Event

- Previously studied: rope reconstruction (Cheng et al. 2014), and reconnection analysis (Dudik et al. 2014).
- The CME was over 1000 km/s in the inner heliosphere, 600 km/s at 1AU (Hess et al. 2014).
- A salient feature was fast-moving flare ribbons which traveled far away from the flare site. These ribbons end up bounding long-lived core-dimming features (D1, D2).

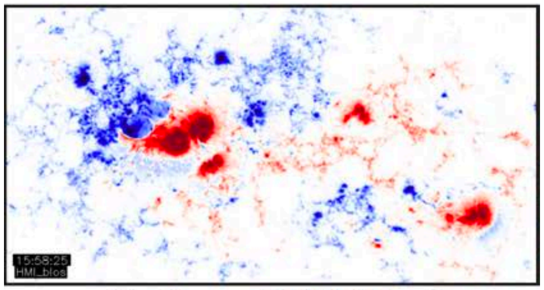

Br (from HMI Blos)

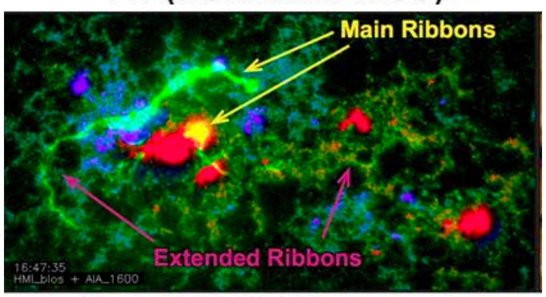

Br + AIA 1600 Ribbons

AIA 193 Base Difference

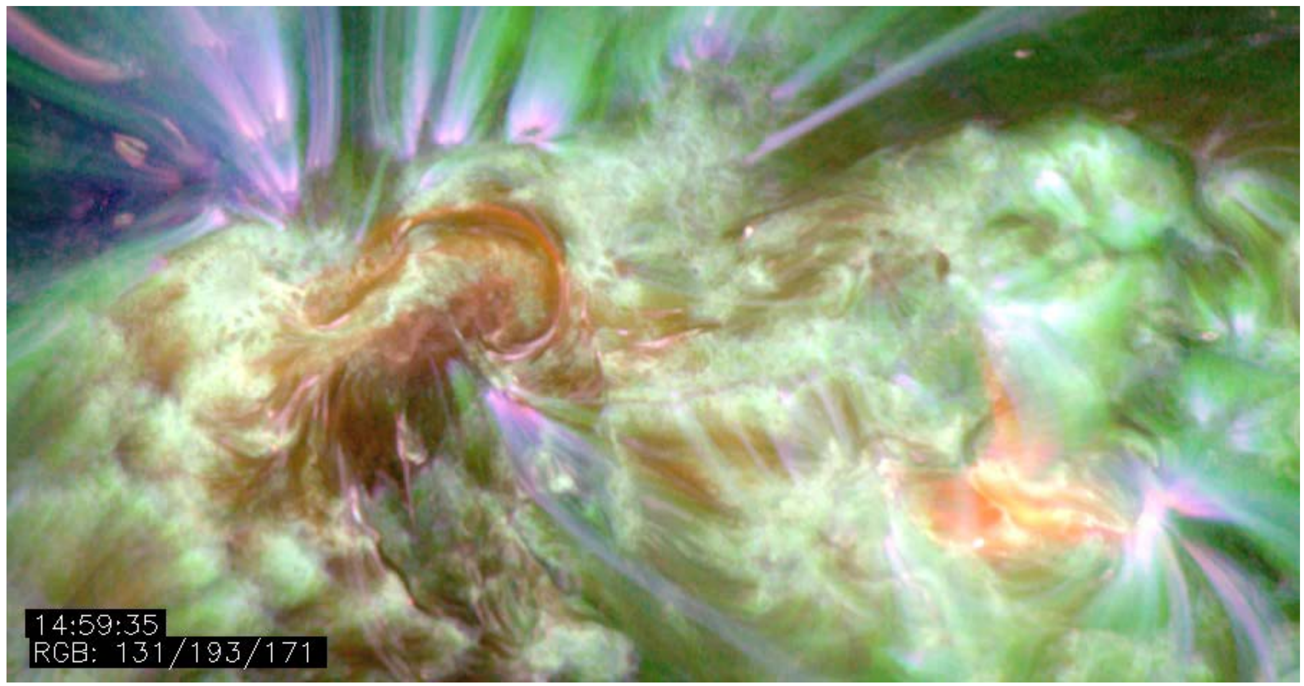

AIA 131 193 171 RGB Composite

12 July 2012: Boundary Conditions

- **Magnetic Map:** full-sun composite tailored for a specific time (2012/07/12 16:00 UT).
  - **Active Region:** Br derived from HMI Vector Camera.
  - **Frontside:** Br derived from 720s HMI LOS Magnetogram.
  - **Farside:** Br from LMSAL Surface Flux Evolution model.

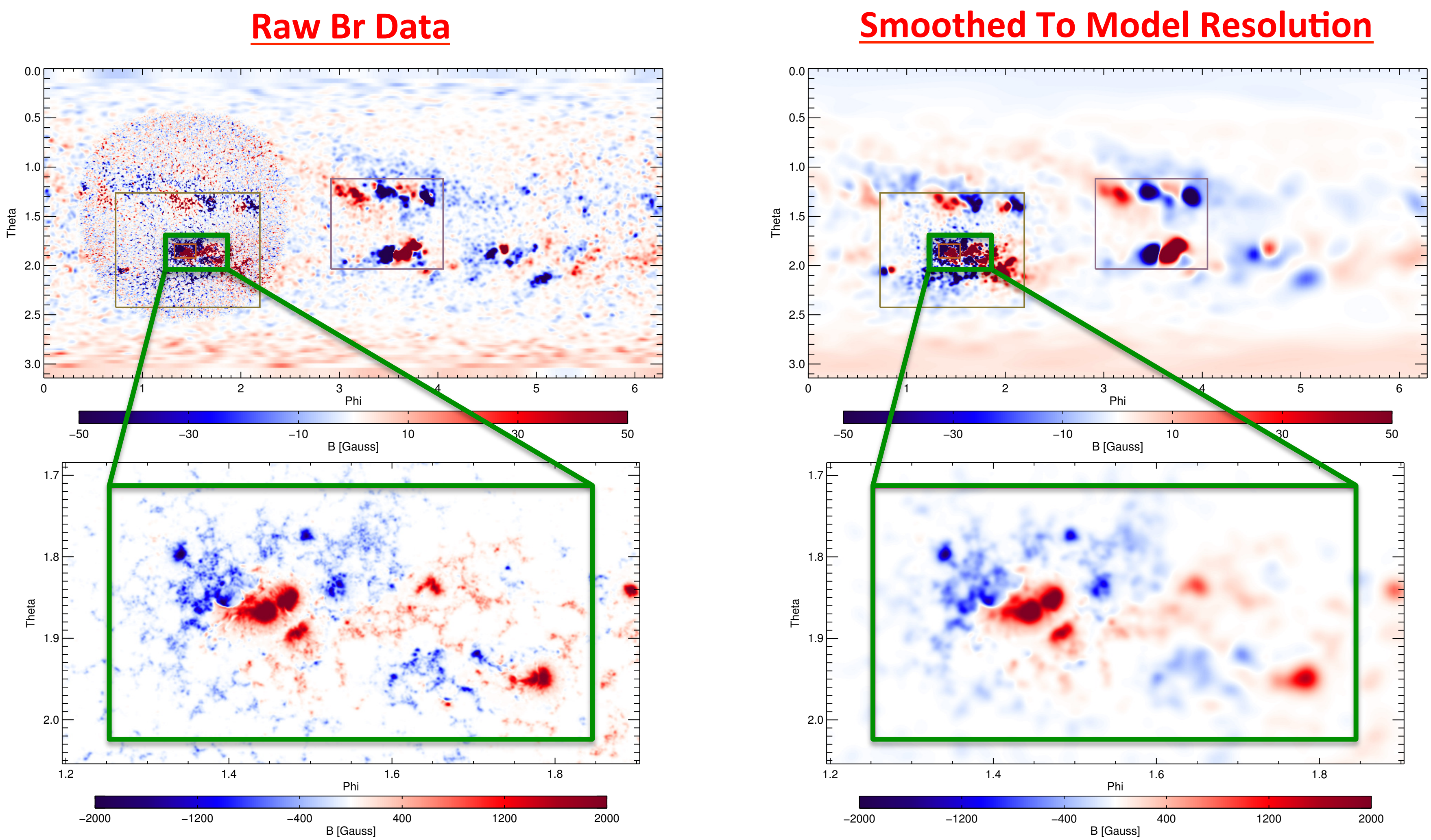

12 July 2012: Thermodynamic MHD Model

- **3D Heating Model:** Wave Turbulence Dissipation (WTD).
    - Heating explicitly set by base field and implicitly by 3D topology (Downs et al. 2016).

Mesh (r,t,p): 392x361x551

Most points concentrated near erupting AR.

Model relaxed for ~40hrs, to build plasma/ solar wind distribution.

Compare Synthetic AIA emission to AIA observations

Observations

Model

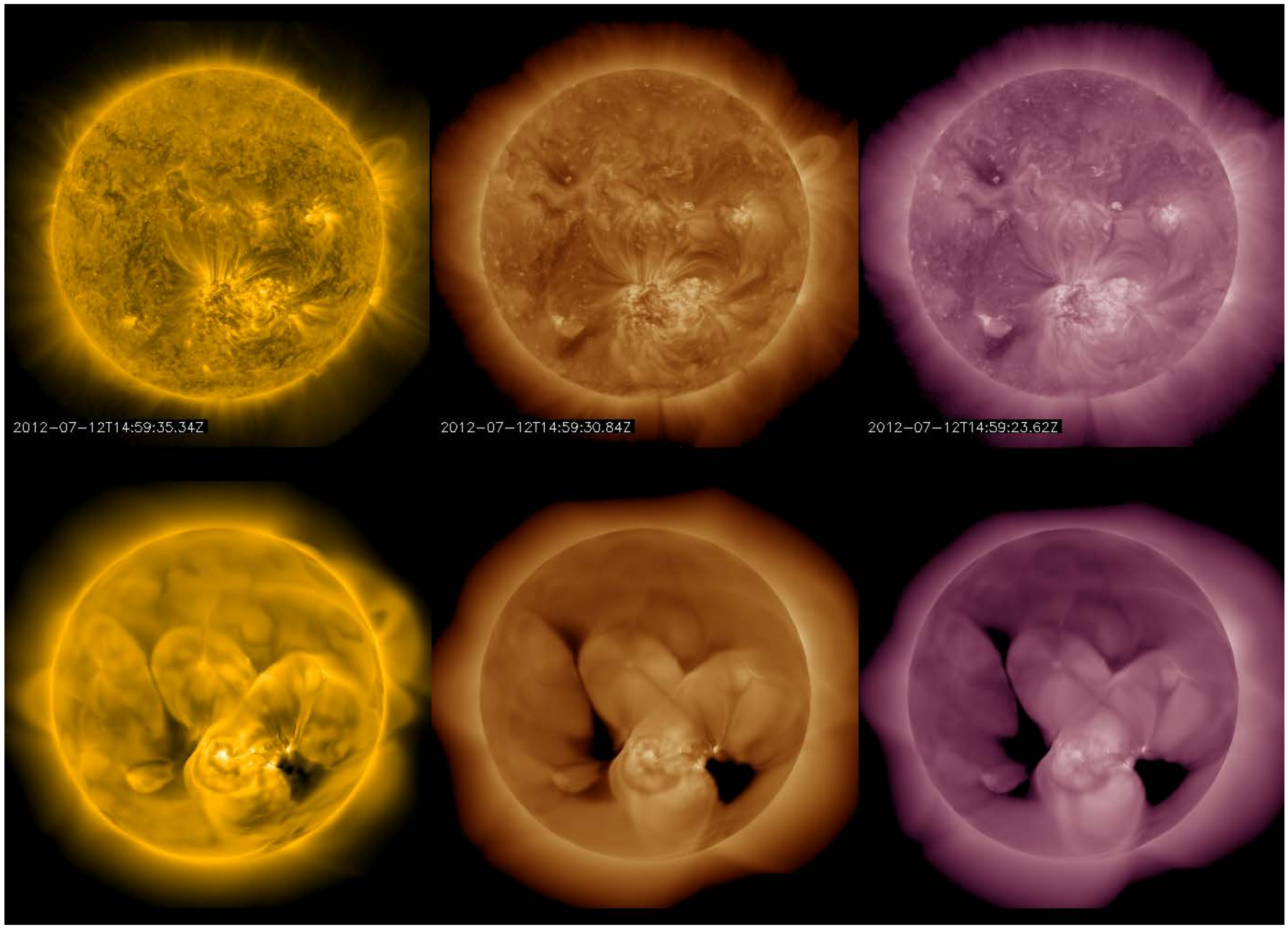

AIA 171 | AIA 193 | AIA 211

Initiating CMEs from other Equilibrium Models

- We have generalized our TDm capability to incorporate other equilibrium models, e.g. nonlinear-force free models (NLFF) developed in other codes
  - Non-trivial because of disparate meshes between codes
  - Must preserve properties to a high degree (e.g., current density **J** in NLFF model)
  - Use radial basis function (RBF) interpolation
  - To preserve **J,** we interpolate **J** onto new mesh and solve elliptic equation to recover vector potential **A** (**J**=curl(**B**), div(**J**)=0)
- July 12, 2012 CME
  - Use NLFF solution with embedded flux rope developed by A. Savcheva, using magnetofrictional method (e.g. Savcheva & van Ballegooijen, ApJ 2009).
  - Solution chosen from several to best match pre-eruptive EUV signatures.

12 July 2012: Inserting a Flux Rope

- NLFF provided by A. Savcheva using CMS magnetofrictional model [van Ballegooijen (2000, 2004, 2007, 2009), Savcheva et al. (2009, 2012a, b, c, 2015, 2016)].
- Relax their model in zero-β MHD, then insert into thermo MHD (slow rise → eruption).

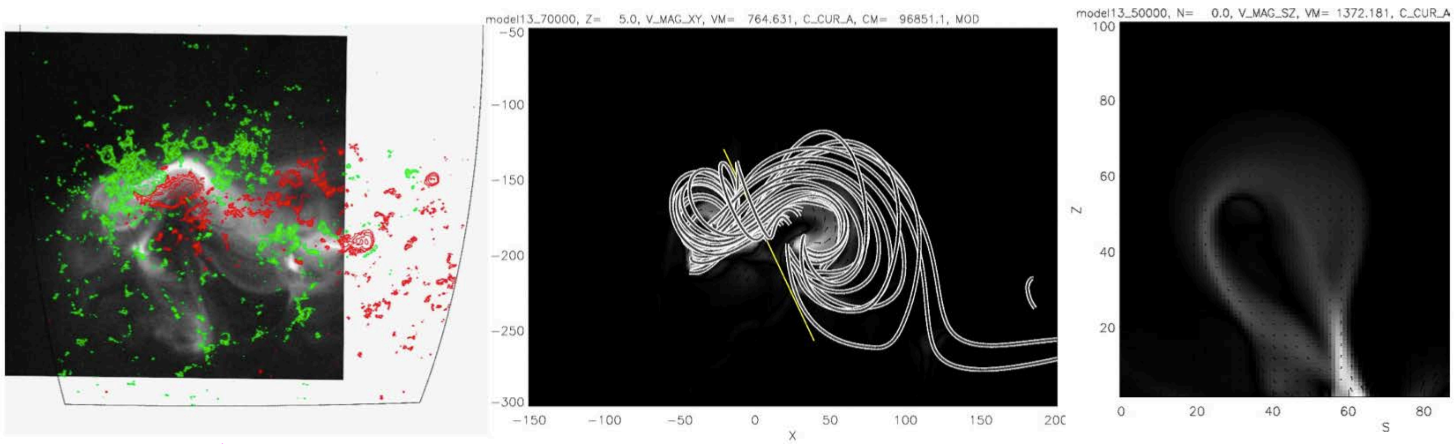

CMS Model
for 12 July 2012

Inserted
Into zero-β
MHD Model
(Relaxation)

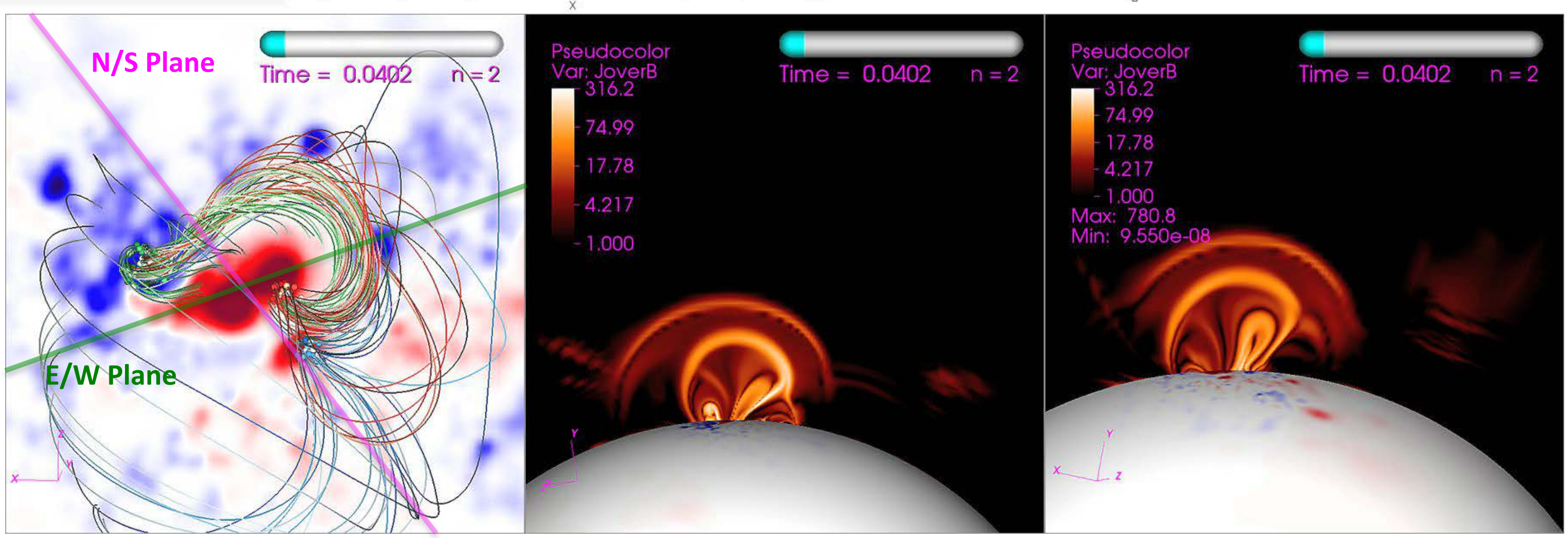

Top View **N/S Plane** **E/W Plane**

12 July 2012: Thermodynamic CME Simulation

- Insert relaxed flux-rope into the thermodynamic MHD model. Multiply the energized field slightly to induce a marginal instability (slow rise, followed by fast reconnection).
- We produce a fast CME (1000+ km/s), large-EUV wave, similar ribbon/dimming features.

Inserted into thermo MHD Model (CME)

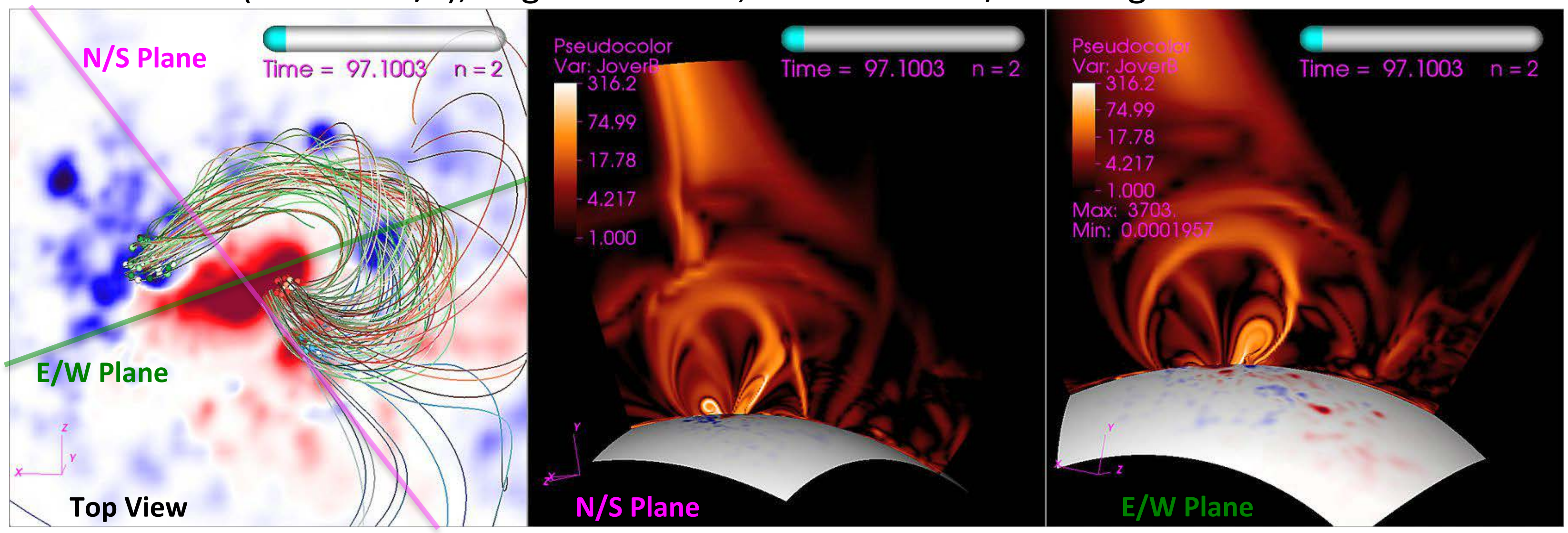

Multi-Band Synthetic Emission

12 July 2012: Thermodynamic CME Simulation

- Synthetic White Light from STEREO-B perspective (AR just behind west limb).
  - CME impulsive early, ~60 degree full width near the end, similar to STB observations.
  - Large-scale wave also visible (simulation is noise free…).

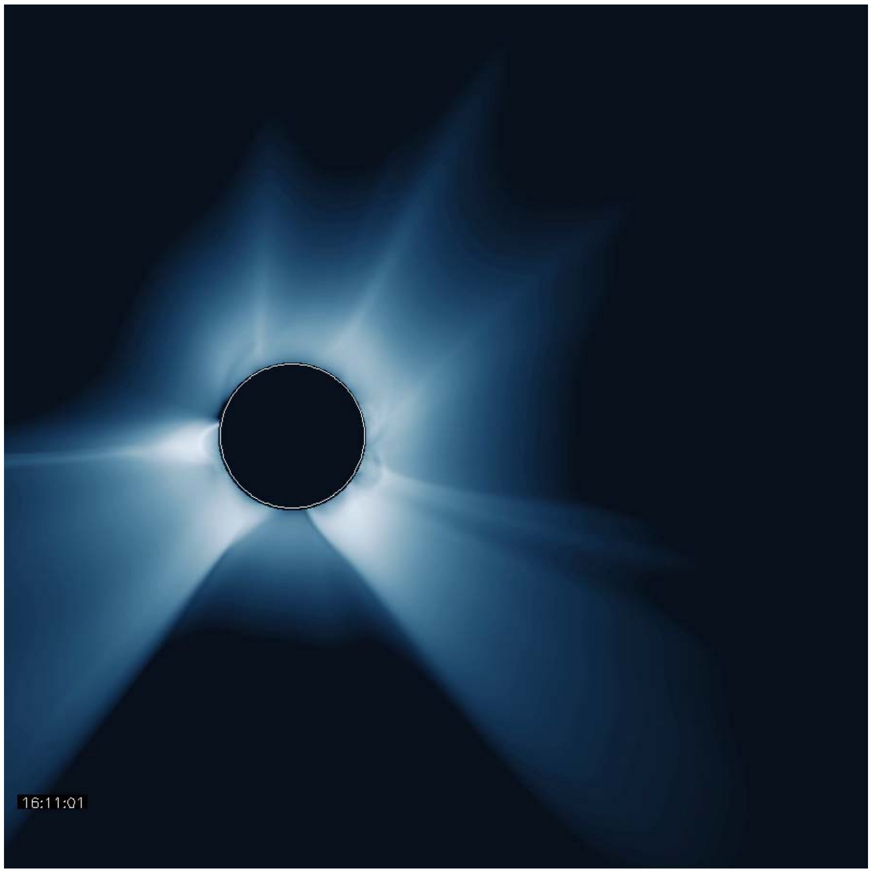

White Light Pb Intensity
(Newkirk Vignetting, Unsharp Masked)

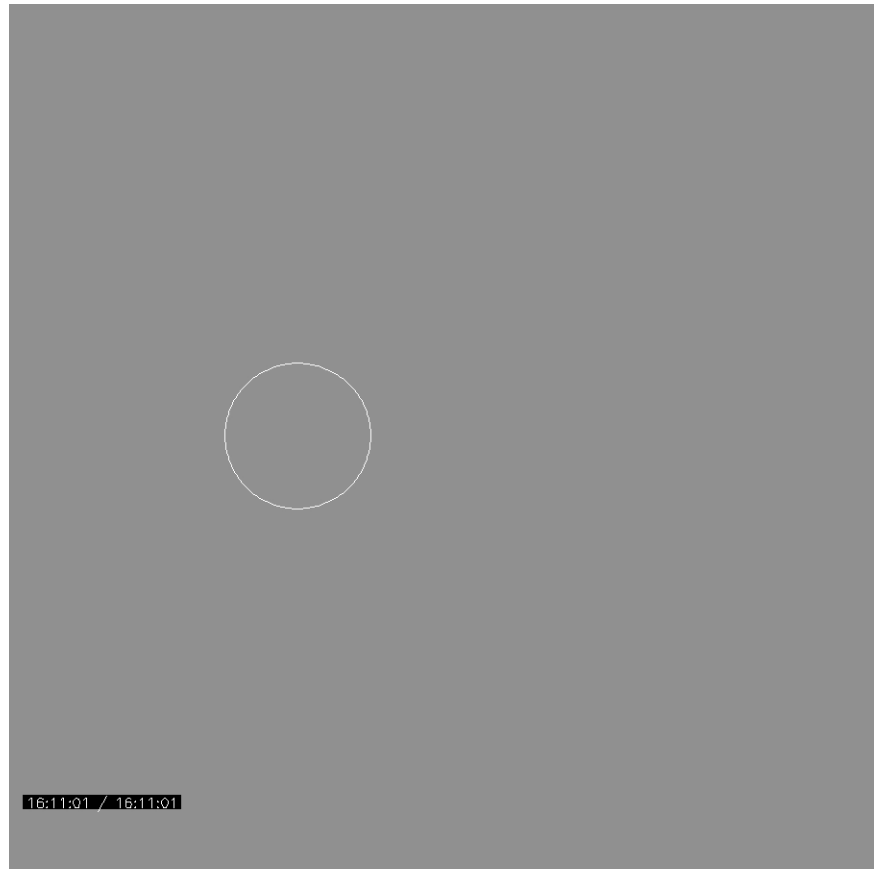

White Light Pb Running Ratio
(2.5 min cadence)

12 July 2012: Thermodynamic CME Simulation

- Full Disk AIA 211 Comparison:
  - Large-scale behavior to south/west is similar.
  - EUV wave is more pronounced in the simulation (linked to CME expansion?)

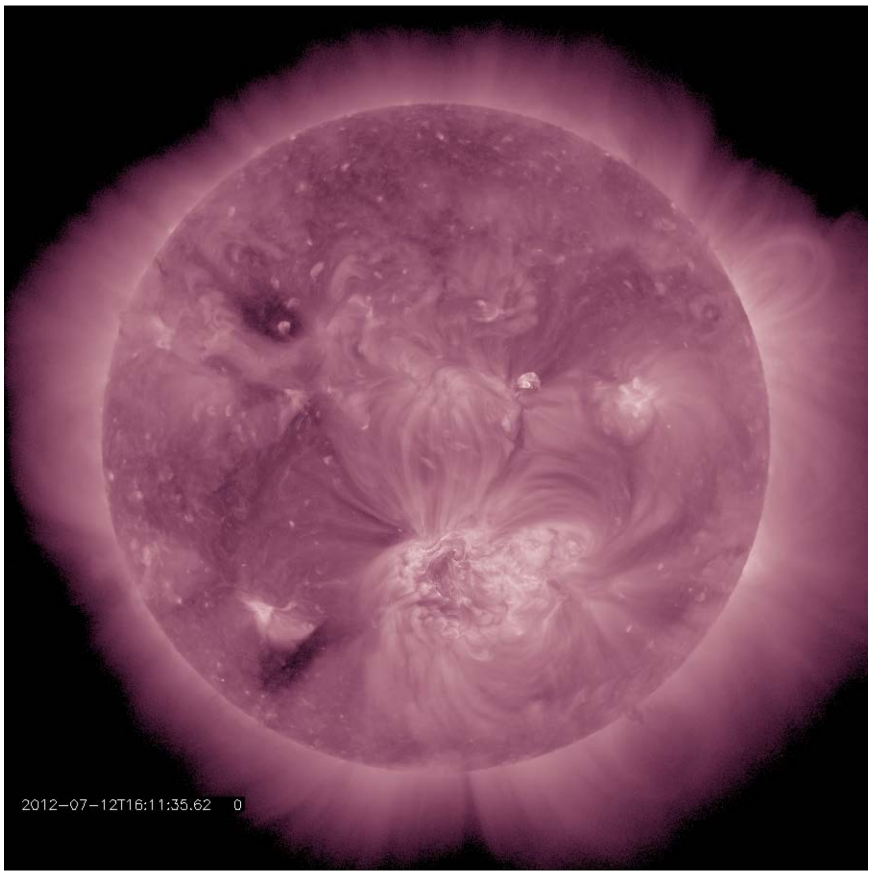

Observations

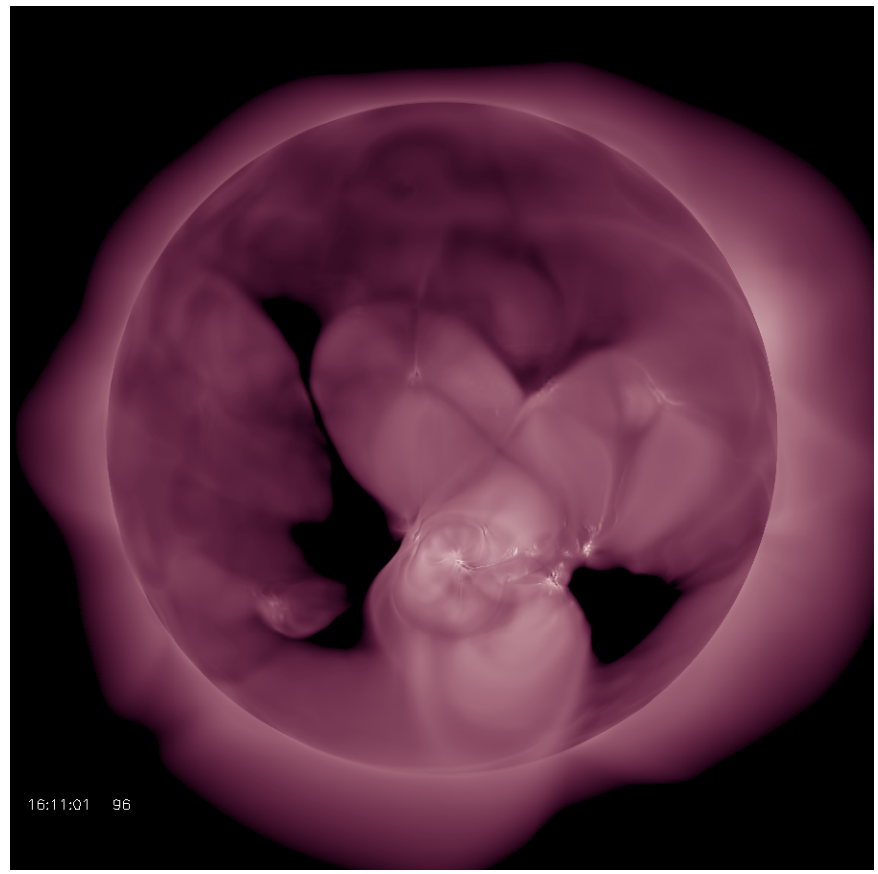

Model

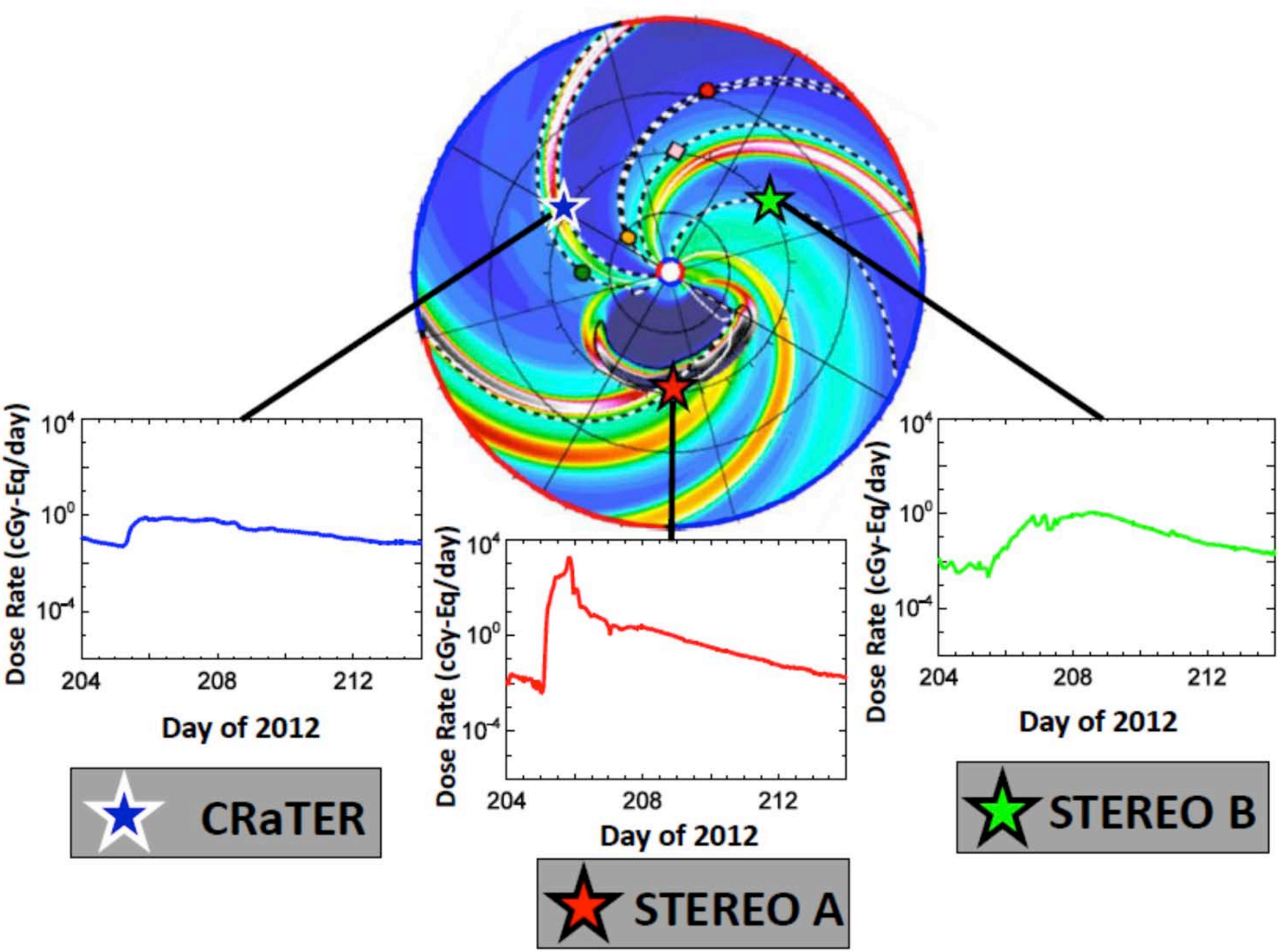

Dose Rate (cGy-Eq/day)
Day of 2012
CRaTER
STEREO A
STEREO B

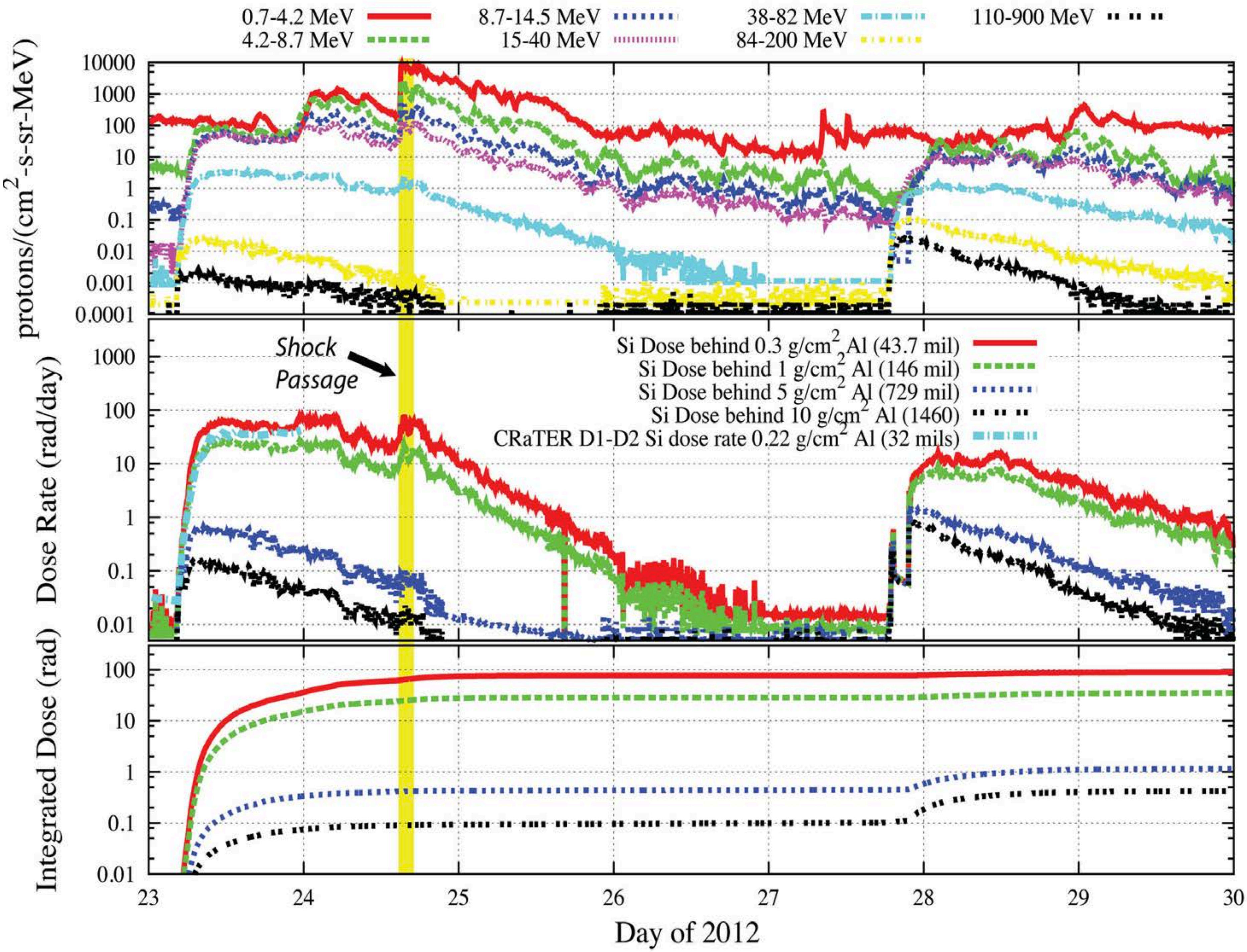

0.7-4.2 MeV
4.2-8.7 MeV
8.7-14.5 MeV
15-40 MeV
38-82 MeV
84-200 MeV
110-900 MeV
protons/(cm2-s-sr-MeV)
Shock Passage
Si Dose behind 0.3 g/cm2 Al (43.7 mil)
Si Dose behind 1 g/cm2 Al (146 mil)
Si Dose behind 5 g/cm2 Al (729 mil)
Si Dose behind 10 g/cm2 Al (1460)
CRaTER D1-D2 Si dose rate 0.22 g/cm2 Al (32 mils)
Dose Rate (rad/day)
Integrated Dose (rad)
Day of 2012

EPREM SEP profiles at different observers (latitude=0°)

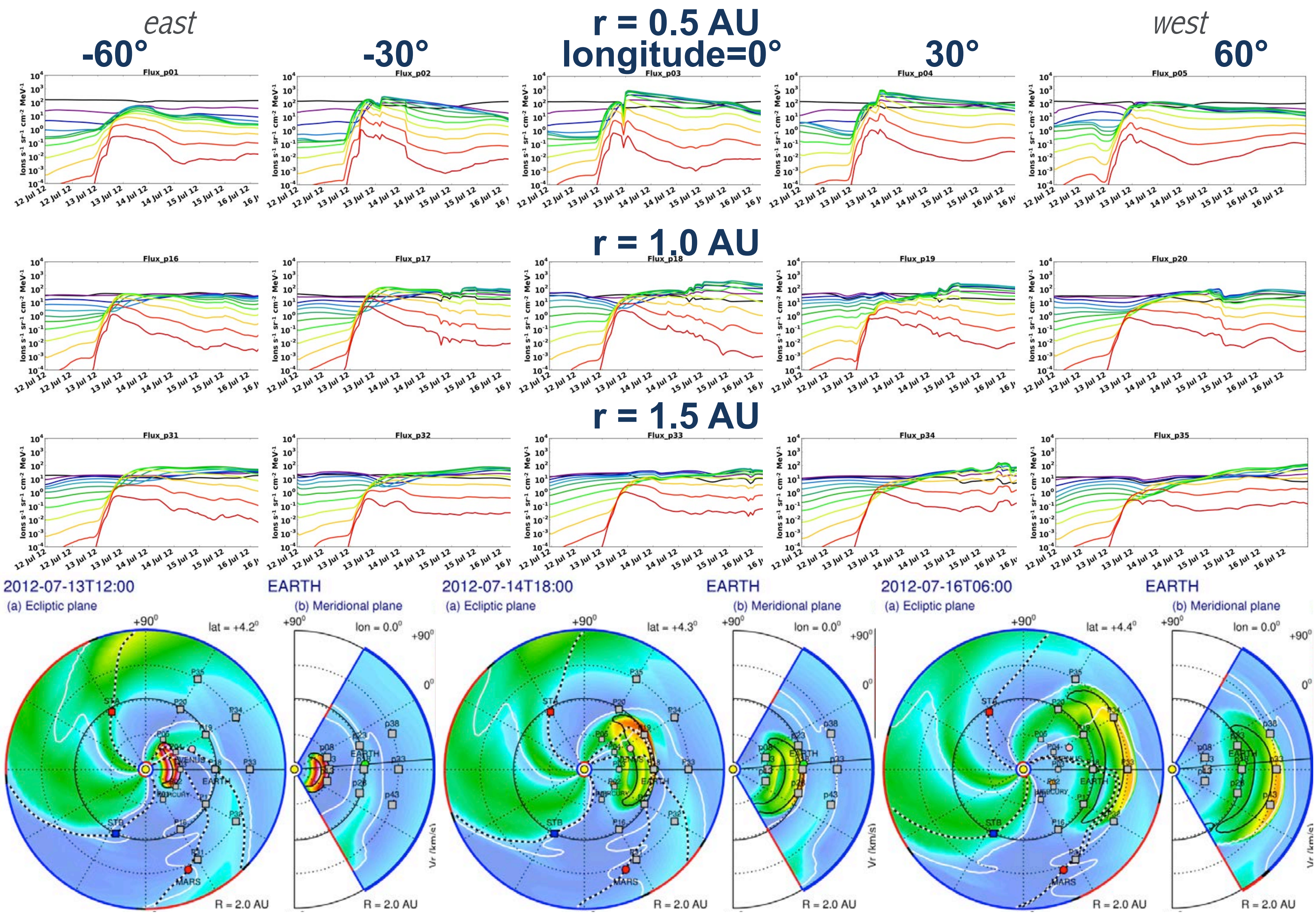

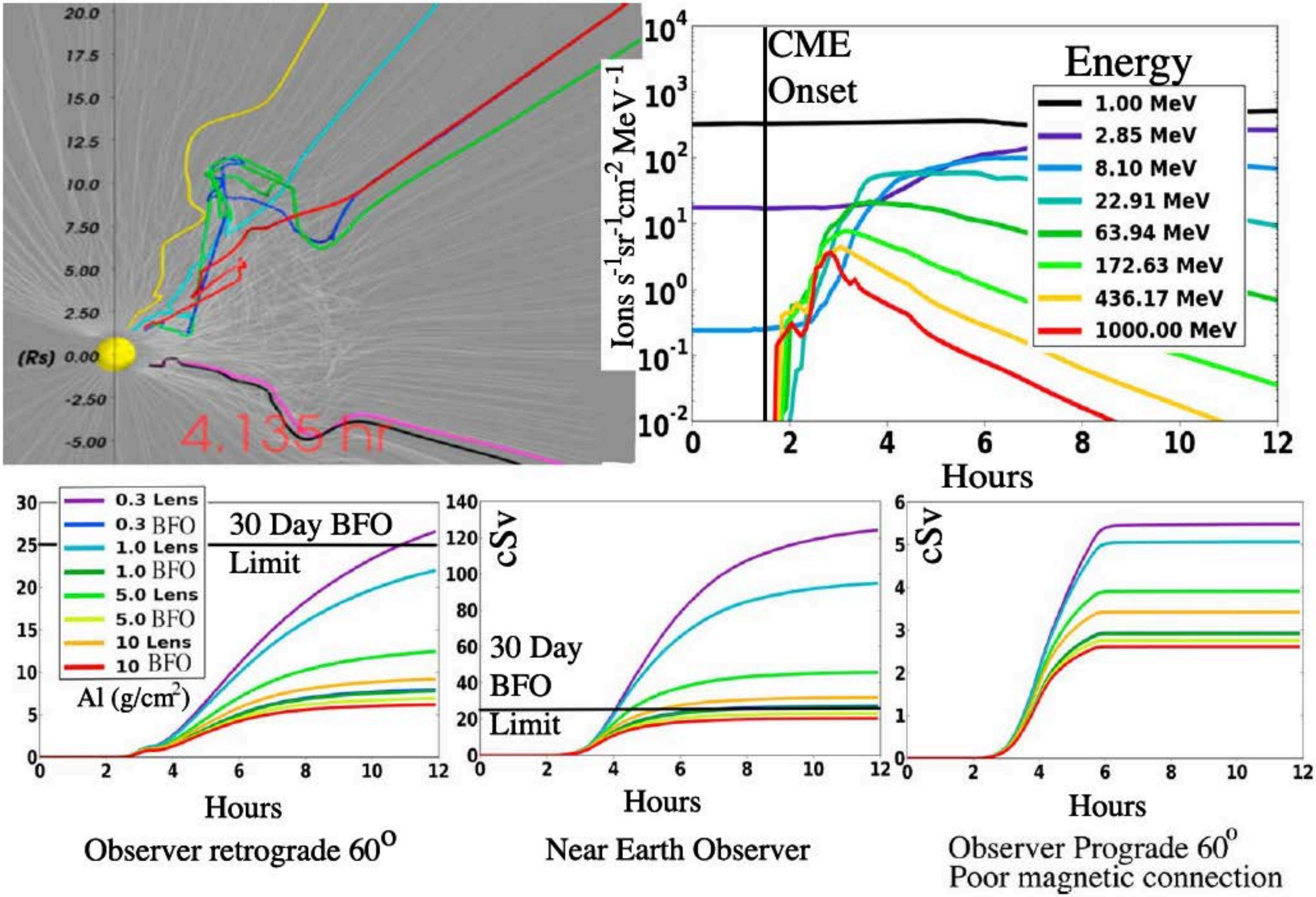
(Rs)
4.135 hr
CME
Onset
Energy
1.00 MeV
2.85 MeV
8.10 MeV
22.91 MeV
63.94 MeV
172.63 MeV
436.17 MeV
1000.00 MeV
Ions s-1sr-1cm-2 MeV-1
Hours
0.3 Lens
0.3 BFO
1.0 Lens
1.0 BFO
5.0 Lens
5.0 BFO
10 Lens
10 BFO
Al (g/cm2)
30 Day BFO
Limit
cSv
30 Day
BFO
Limit
Hours
Observer retrograde 60o
Near Earth Observer
Observer Prograde 60o
Poor magnetic connection

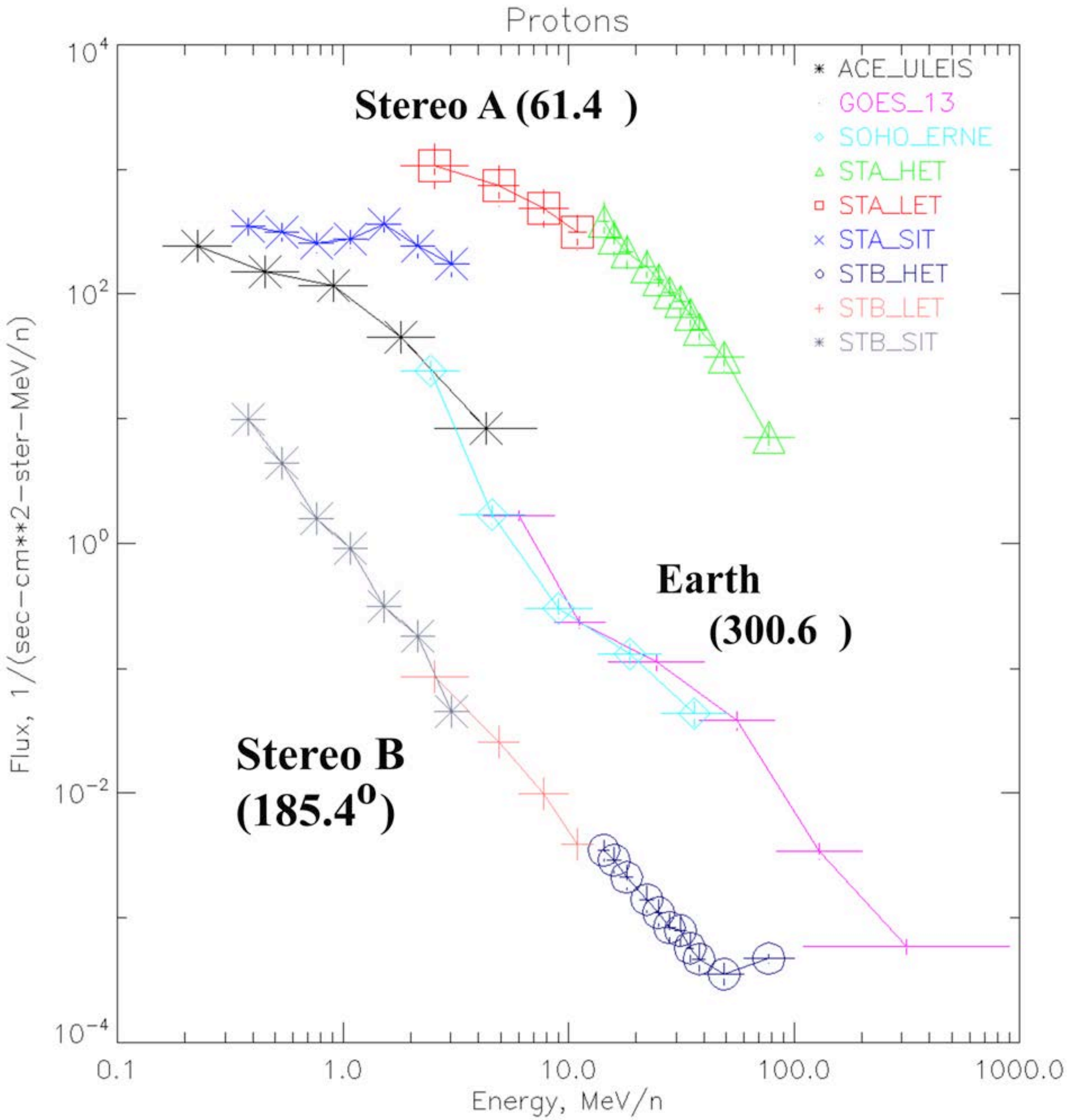
Protons
ACE_ULEIS
GOES_13
SOHO_ERNE
STA_HET
STA_LET
STA_SIT
STB_HET
STB_LET
STB_SIT
Stereo A (61.4)
Earth
(300.6)
Stereo B
(185.4°)
Flux, 1/(sec-cm**2-ster-MeV/n)
Energy, MeV/n
0.1
1.0
10.0
100.0
1000.0

Carrington Event?!

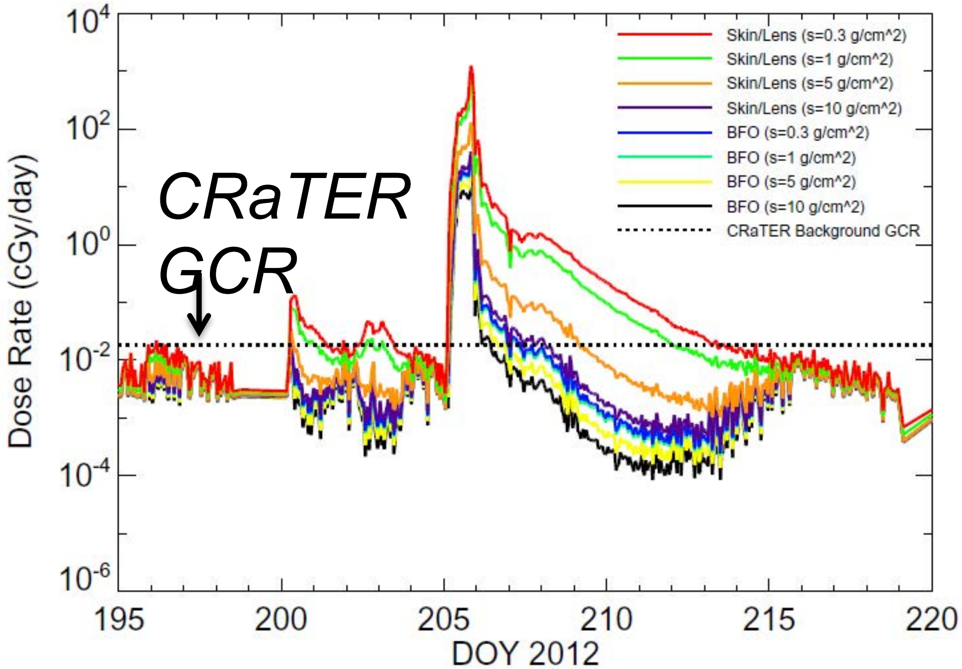

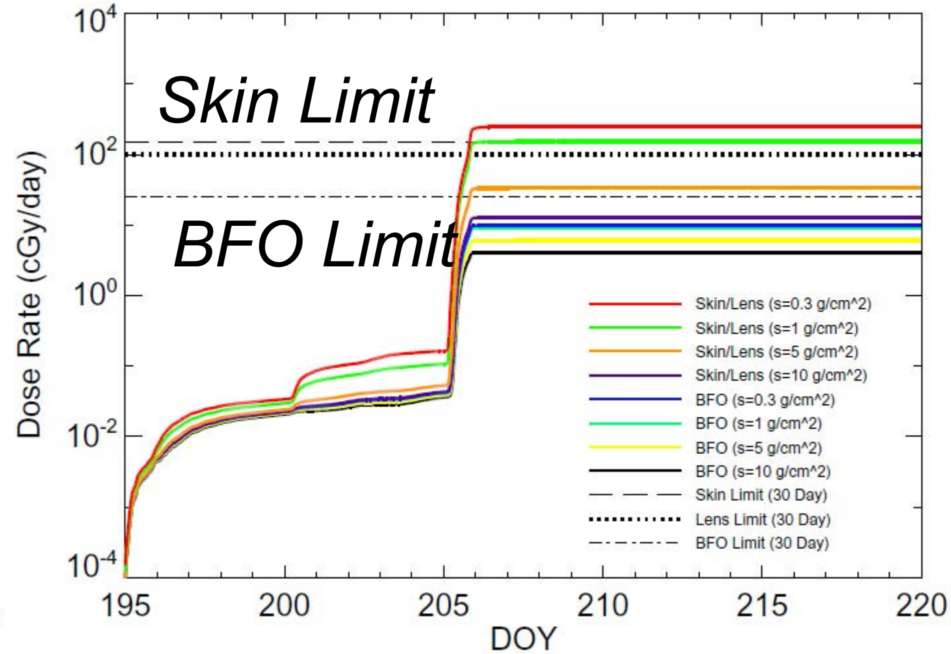

- Dose rate for skin/eye and BFO for four different levels of shielding which correspond to spacesuit, heavy spacesuit, spacecraft and heavy protective shielding.
- Average background GCR dose rate measured by CRaTER during this time is also shown.
- NASA 30 day dose limits for skin and eye exceeded for both levels of spacesuit shielding and the heaviest shielding reduces the total accumulated dose by more than an order of magnitude.
- BFO limit is not exceeded for any level of shielding, though we see that heavier shielding is less effective at reducing the total dose.

Summary

- Previously, we have used TDm flux ropes to realistically model CME events with themodynamic MHD simulations
- We have extended this capability to insert other equilibria (e.g., NLFF solutions) into MHD models
- We now have a working model/simulation of the 12 July 2012 CME
- Analysis is just beginning. Further work:

  - How does the flux-rope interact with and reconnect with the surrounding field?
  - What role does the quadrupolar topology play in this reconfiguration?
  - How are the dimming regions/ribbons related to flux-rope connectivity?
  - How does the flux-rope evolve over time in the heliosphere?
  - Coupling with EMMREM to explore SEP acceleration and transport for this event

Extra Slides

12 July 2012: Thermodynamic CME Simulation

- Zoomed in AIA 211/Field Mapping Comparison:
  - Large-scale flare/dimming ribbons light up in similar manner.
  - The erupting rope rapidly reconnects with the overlying field lobes.
  - Visualize by looking at high-Q lines determined from field-line mapping.

Observations

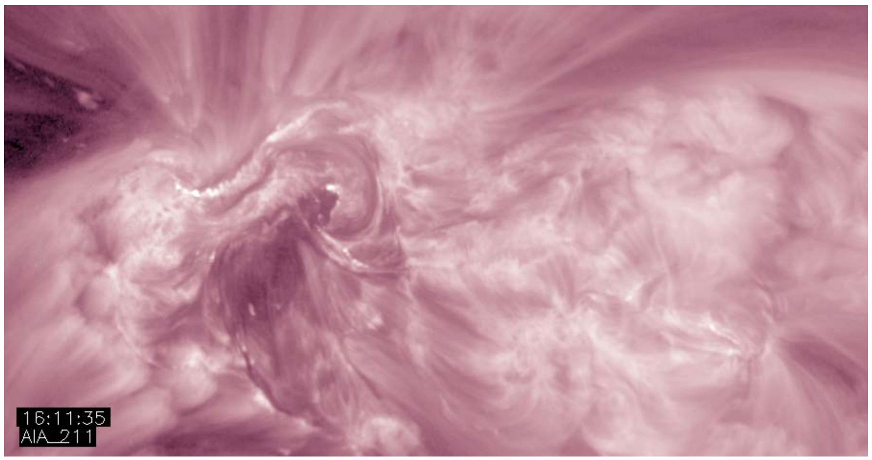

Model

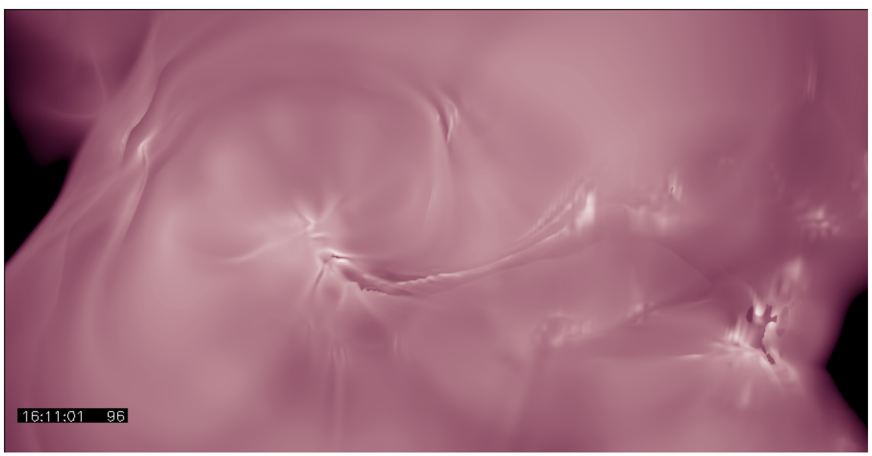

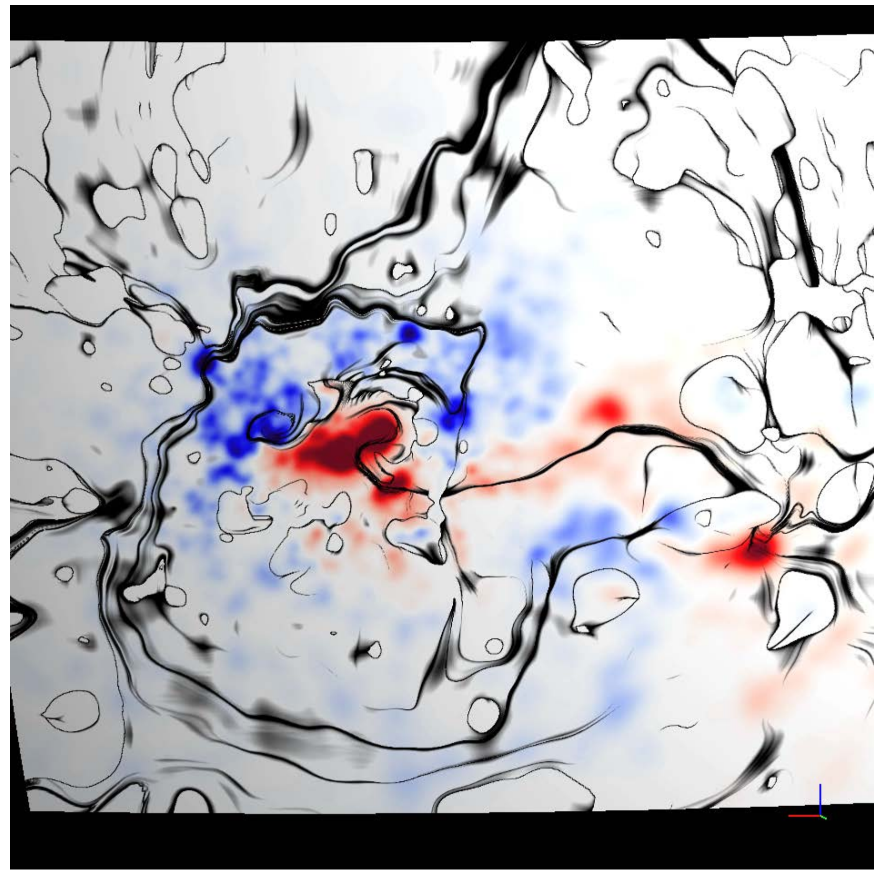

Model Br (red/blue) + $\log_{10}$ Q (black)

MHD Equations: MAS/CORHEL

$$\nabla \times \mathbf{A} = \mathbf{B},$$

$$\frac{\partial \mathbf{A}}{\partial t} = \mathbf{v} \times \mathbf{B} - \frac{c^2 \eta}{4\pi} \nabla \times \mathbf{B},$$

$$\frac{1}{\gamma - 1} \left(\frac{\partial T}{\partial t} + \mathbf{v} \cdot \nabla T \right) = -T \nabla \cdot \mathbf{v} - \frac{m_p}{2k\rho} (\nabla \cdot \mathbf{q} + n_e n_p Q(T) - H_{\rm ch}),$$

$$\frac{\partial \rho}{\partial t} + \nabla \cdot (\rho \mathbf{v}) = 0,$$

$$\rho \left(\frac{\partial \mathbf{v}}{\partial t} + \mathbf{v} \cdot \nabla \mathbf{v} \right) = \frac{\nabla \times \mathbf{B} \times \mathbf{B}}{4\pi} - \nabla p - \nabla p_w + \rho \mathbf{g} + \nabla \cdot (\nu \rho \nabla \mathbf{v}),$$

$$\gamma = 5/3,$$

$$\mathbf{q} = \begin{cases} -\kappa_0 T^{5/2} \hat{\mathbf{b}} \hat{\mathbf{b}} \cdot \nabla T & \text{if } R_\odot \le r \lesssim 10 R_\odot \\ \alpha n_e k T \mathbf{v} & \text{if } r \gtrsim 10 R_\odot \end{cases} ,$$

- Alfven wave pressure $p_{\rm w}$ evolution advanced with WKB or WTD equations
- Empirical coronal heating H_{CH} (Lionello et al 2009) or from WTD equations

TD Flux Rope

Titov & Démoulin 1999

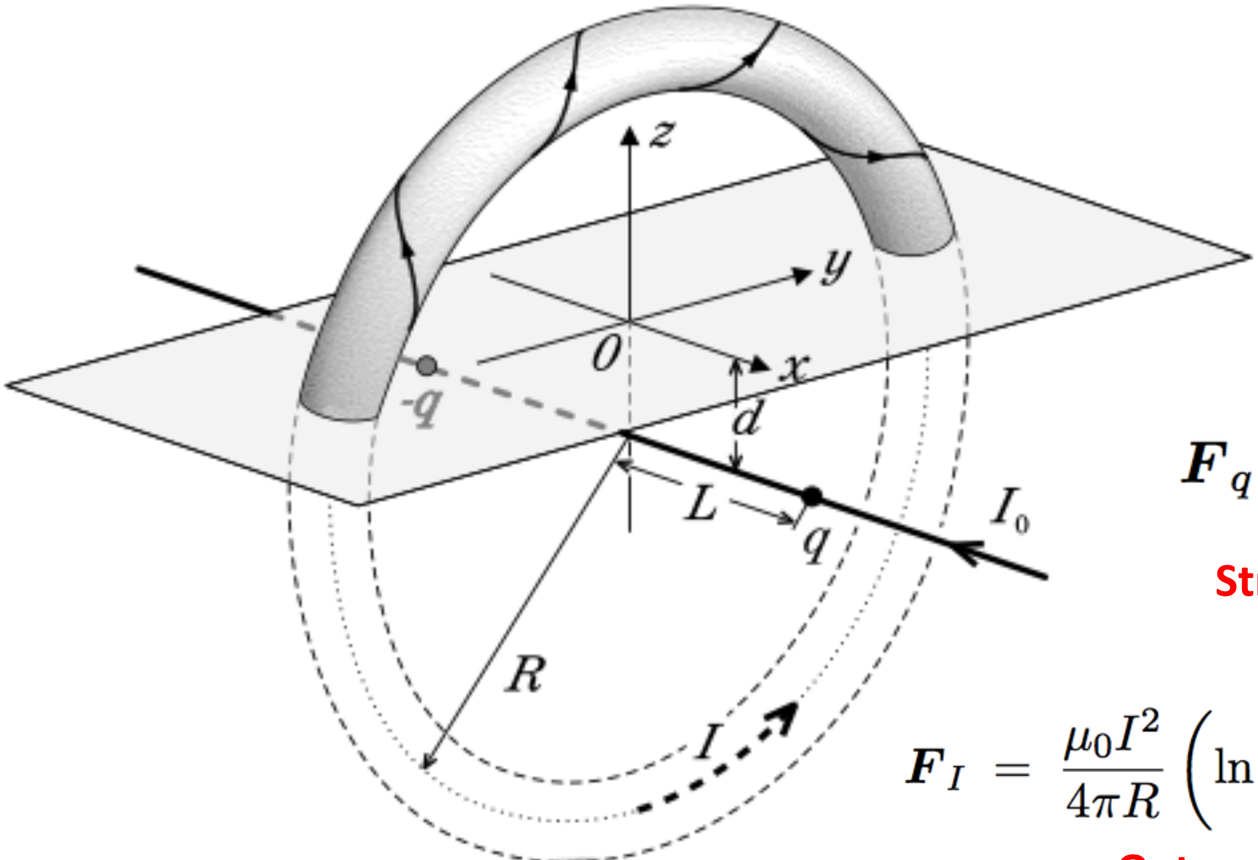

$$\boldsymbol{F}_q = -\frac{2qLI\boldsymbol{n}}{(R^2+L^2)^{3/2}},$$

Strapping force from charges

$$\boldsymbol{F}_I = \frac{\mu_0 I^2}{4\pi R}\left(\ln\frac{R}{a} + \ln 8 - 3/2 + l_{\mathrm{i}}/2\right)\boldsymbol{n}$$

Outward force of the Rope

- Analytic model or circular flux rope as current carrying ring + axial field
- Know the hoop force of flux rope
- This force is balanced by a strapping field

TDm Flux Rope

Titov et al. 2014

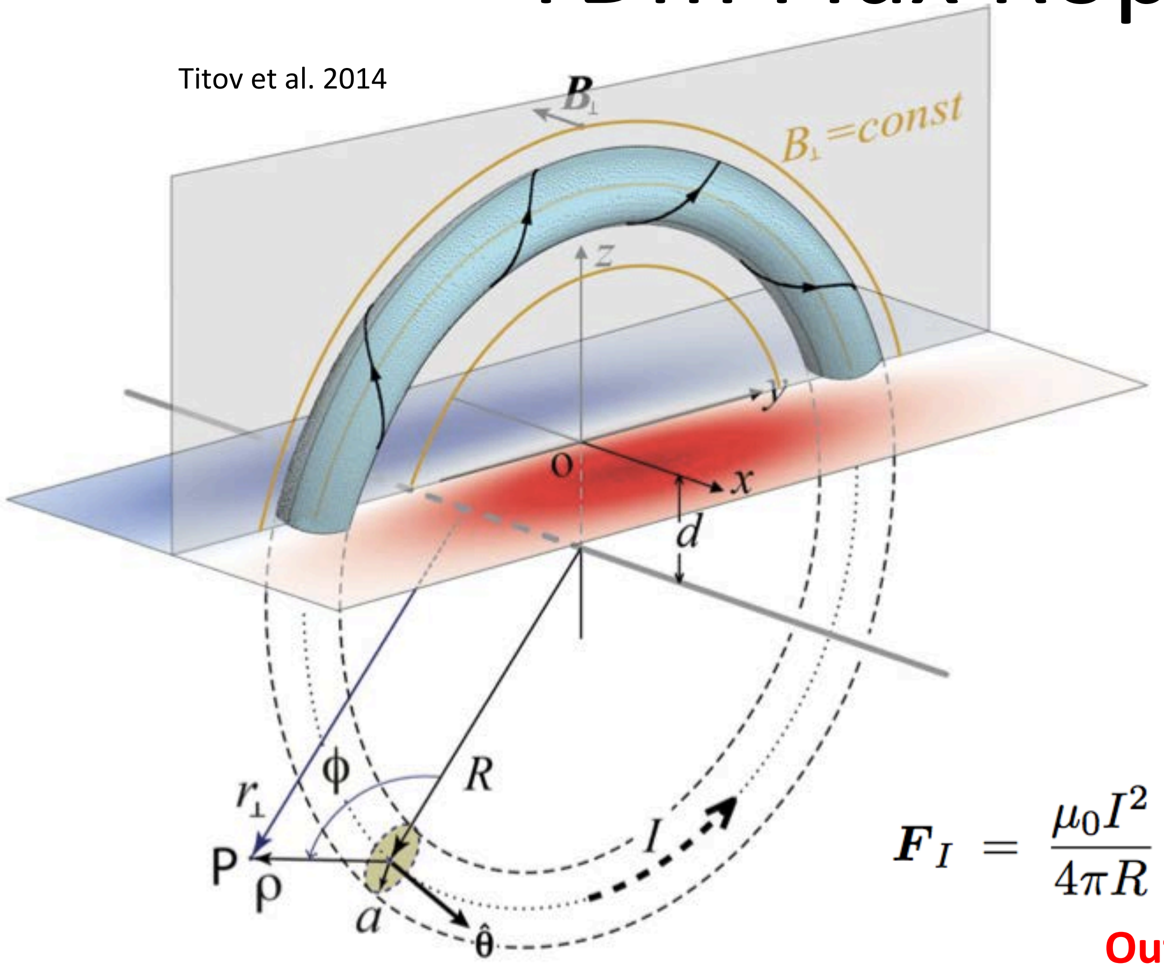

Instead you can use the arcade of the AR you want to study

$$F_q = -\frac{2qLI\boldsymbol{n}}{(R^2 + L^2)^{3/2}},$$

Strapping force from charges

$$\boldsymbol{F}_I = \frac{\mu_0 I^2}{4\pi R}\left(\ln\frac{R}{a} + \ln 8 - 3/2 + l_\mathrm{i}/2\right)\boldsymbol{n}$$

Outward force of the Rope

- Complete expression for rope vector potentials given in Titov et. al 2014.
- Two types of volumetric current profiles considered (hollow core, parabolic)
- This model is implemented in the MAS code and can be inserted into any configuration